Sheaths: More complicated than you think[a)]

Noah Hershkowitz[b)]
University of Wisconsin-Madison, Madison, Wisconsin 53706

(Received 7 December 2004; accepted 7 February 2005; published online 9 May 2005)

Sheaths in low temperature collisionless and weakly collisional plasmas are often viewed as simple examples of nonlinear physics. How well do we understand them? Closer examination indicates that they are far from simple. Moreover, many predicted sheath properties have not been experimentally verified and even the appropriate "Bohm velocity" for often encountered two-ion species plasma is unknown. In addition, a variety of sheathlike structures, e.g., double layers, can exist, and many two- and three-dimensional sheath effects have not been considered. Experimental studies of sheaths and presheaths in weakly collisional plasmas are described. A key diagnostic is emissive probes operated in the "limit of zero emission." Emissive probes provide a sensitive diagnostic of plasma potential with a resolution approaching 0.1 V and a spatial resolution of 0.1 cm. Combined with planar Langmuir probes and laser-induced fluorescence, they have been used to investigate a wide variety of sheath, presheath, and sheathlike structures. Our experiments have provided some answers but have also raised more questions. © *2005 American Institute of Physics*.
[DOI: 10.1063/1.1887189]

I. INTRODUCTION

Sheaths are non-neutral regions that normally form at plasma boundaries to balance electron and ion losses. They are one of the most prominent and well-known features of confined plasma. Sheaths matter. In low temperature plasma, sheaths are critical to providing directed ion energy for directional etching in the fabrication of semiconductor devices. In high temperature plasma, sheaths determine the details of wall heating, erosion, and wall material recycling. Knowledge of sheaths is important to the understanding of plasma wall interactions, Langmuir probe characteristics, plasma etching, spacecraft charging, etc. Sheaths in unmagnetized collisionless plasma are often viewed as a simple example of nonlinear physics. But are they simple, and how well do we understand them? Examination of the literature on sheaths indicates that they are far from simple and that many predicted sheath properties have not been experimentally verified. In addition, a variety of sheathlike structures—double sheaths and double layers—can exist. Ions require a finite (Bohm) velocity at the sheath boundary. Experimental studies of sheaths' and presheaths' potential drop required to accelerate ions to the Bohm are described.

II. THEORETICAL CONSIDERATION

A. Derivation of sheaths

The usual derivation of the sheath potential profile considers space charge limited emission.[1] Ions or electrons originate from a sheath boundary where the electric field equals zero. Consider an ion source at $x=0$, $\phi=0$, assume the electric field $E_0=-d\phi/dx=0$, the velocity $v_0\approx 0$, and $\phi=-V$ at x. We can express the ion density $n_i(x)$ by

$$n_i(x)=\frac{J_0}{ev(x)}=\frac{J_0}{e\left(\frac{-2e\phi}{m_i}\right)^{1/2}}, \tag{1}$$

where J_0 is the ion current density at the boundary. If no electrons are assumed, Poisson's equation gives

$$\frac{d^2\phi}{dx^2}=-\frac{ne}{\varepsilon_0}=-\frac{J_0}{\varepsilon_0\left(\frac{-2e\phi}{m_i}\right)^{1/2}}. \tag{2}$$

Multiplying by $d\phi/dx$ and integrating twice gives the Child–Langmuir law.

$$J_0=\frac{\varepsilon_0\left(\frac{2e}{m_i}\right)^{1/2}\frac{4}{9}V^{3/2}}{x^2}. \tag{3}$$

Note that zero initial velocity has been assumed at $x=0$ and electrons are ignored. These assumptions limit the application of this result to potentials which satisfy $eV/T_e\gg 1$, with the electron temperature in units of eV.

Langmuir[2] recognized that ions in plasma required a finite velocity directed into the sheath at the sheath boundary and Bohm[3] showed that the directed velocity needed to satisfy $v\geqslant c_s\approx\sqrt{(\gamma_i T_i+T_e)/m_i}$. The directed velocity must exceed the "Bohm velocity" c_s that also equals the ion acoustic wave velocity. Following Stangeby and Chankin,[4] the Bohm criterion can be derived as follows: The Boltzmann relation for (isothermal) electrons gives

$$\frac{dn_e}{dx}=\frac{en_e}{T_e}\frac{d\phi}{dx}=-\frac{en_e}{T_e}E, \tag{4}$$

where E is electric field. Assuming T_i to be constant, conservation of ion flux and one-dimensional behavior, the ion fluid equations can be written

[a)]Paper MR1 1, Bull. Am. Phys. Soc. **49**, 246 (2004).
[b)]Maxwell Prize speaker.

$$\frac{d}{dx}(n_i v_i) = 0, \tag{5}$$

$$n_i m_i v_i \frac{dv_i}{dx} = -\frac{dp_i}{dx} + eEn_i. \tag{6}$$

Taking $dp_i/dx = dn_i/dx\,\gamma_i T_i$ and combining Eqs. (4)–(6) gives

$$\left(v^2 - \frac{\gamma_i T_i + T_e\left(\frac{dn_e}{dx}\Big/\frac{dn_i}{dx}\right)\frac{n_i}{n_e}}{m_i}\right)\frac{dn_i}{dx} = 0. \tag{7}$$

Equation (7) is satisfied in the bulk plasma, where $n_e = n_i$ and $dn_i/dx = dn_e/dx = 0$. At the sheath edge, assuming $n_e = n_i$, and

$$\frac{dn_i}{dx} = \frac{dn_e}{dx} \neq 0, \tag{8}$$

$$v_i^2 = \frac{\gamma_i T_i + T_e}{m_i} \equiv c_s^2. \tag{9}$$

The assumption $dn_e/dx \neq 0$ is equivalent to assuming that $E \neq 0$. The plasma potential in the ion sheath must have negative curvature. Poisson's equation gives $n_i \geqslant n_e$ throughout the ion sheath so

$$\frac{dn_i}{dx} \leqslant \frac{dn_e}{dx} \tag{10}$$

at the sheath edge. Thus the ion drift velocity must be at least as large as the Bohm velocity c_s.

If we take

$$J_0 = \alpha_i n_{i0} e \sqrt{\frac{T_e}{m_i}}, \tag{11}$$

where n_{i0} is the density in the bulk plasma, $\alpha_i n_{i0}$ is the ion density at the sheath boundary, and $T_e \gg T_i$ is assumed,

$$\alpha_i n_0 e^2 \left(\frac{T_e}{m_i}\right)^{1/2} T_e = \frac{\varepsilon_0 T_e \left(\frac{2e}{m_i}\right)^{1/2} \frac{4e}{9} V_0^{3/2}}{s^2}, \tag{12}$$

$$\frac{s}{\lambda_D} = \frac{0.79}{\sqrt{\alpha_i}}\left(\frac{eV_0}{T_e}\right)^{3/4}, \tag{13}$$

where λ_D is the Debye length and $-V_0$ is the bias voltage on the boundary. Equation (13) gives the "Child–Langmuir" sheath. The length s can be identified as the sheath thickness. It is apparent that the ion sheath thickness is proportional to the Debye length in weakly collisional systems with $eV_0/T_e \gg 1$. The Debye length is normally much smaller than the plasma dimensions L.

B. Presheath

Acceleration to the Bohm velocity in weakly collisional plasma requires an axial potential profile connecting the sheath to the bulk plasma. This region can be identified to be the Bohm presheath. Assuming a collisionless presheath, ion energy conservation, quasineutrality, and electrons satisfying the Boltzmann relation, a potential drop of $e\Delta\phi = -T_e/2$ is required to give ions starting at rest enough energy to reach the Bohm velocity where n_0 is the bulk plasma density.

The density at the sheath edge is

$$n = n_0 \exp\left(\frac{e\Delta\phi}{T_e}\right) = 0.61 n_0. \tag{14}$$

The presheath potential drop $\Delta\phi$ increases when collisions are present,[5,6] so α_i is normally smaller than 0.61.

Riemann[7] has shown that when ionization can be neglected and when the ion-neutral collision cross section is either independent of v or proportional to $1/v$, the plasma potential in the presheath varies as

$$\frac{e(\phi - \phi_0)}{T_e} = \sqrt{\frac{x - x_0}{\lambda_c}}, \tag{15}$$

where λ_c is the ion-neutral collision mean free path. The derivation of the Child–Langmuir sheath assumed the electric field at the sheath edge equals 0. On the other hand, Eq. (15) suggests that $E \to \infty$ at x_0. How big is E at the presheath/sheath boundary x_0? Godyak[8] has argued the electron density has a scale length the order of the local Debye length so Eq. (4) gives $E \approx T_e/e\lambda_D$. Godyak argued that $E = T_e/e\lambda_D$ is the appropriate sheath boundary condition. The electrons must be considered when eV/T_e is not much greater than 1.0. When the boundary potential is in this range, the sheath is often referred to as a Debye sheath. The plasma potential profile depends on the details of the electron and ion velocity distribution functions at the sheath boundary. In this paper, it is assumed that $eV_0/T_e \gg 1$. In this case, the region in which the electron density is reduced to a negligible value is identified as the transition region.

C. Electron sheaths

The result given by Eq. (13) is independent of mass and similar results can be derived for electron sheaths that contain no ions. Ion sheaths are well known while electron sheaths in weakly collisional low temperature plasma are only common near Langmuir probes biased to collect electron saturation current. Identifying J_{0e} as the random electron flux directed toward the sheath at the sheath edge

$$J_{0e} = \alpha_e \frac{n_{0e} e}{4} \sqrt{\frac{8T_e}{\pi m_e}} \tag{16}$$

gives

$$\frac{s}{\lambda_D} = \frac{0.32}{\sqrt{\alpha_e}}\left(\frac{eV_0}{T_e}\right)^{3/4}. \tag{17}$$

In many situations a potential dip forms between the bulk plasma and the electron sheath. The potential minimum serves as a virtual anode. The presence of the potential dip $\Delta\phi_{\mathrm{dip}}$ reduces the electron sheath current density to

$$\alpha_e = \exp\left(\frac{-e\Delta\phi_{\mathrm{dip}}}{T_e}\right). \tag{18}$$

In weakly collisional plasma, ion sheaths are normally found at the boundaries. The plasma potential is more positive than most positively biased electrode. Electron sheaths are nor-

mally only present near small probes when they are biased more positive than the plasma potential or at electron emitting surfaces. In high-pressure collisional plasma, such as those used in lighting, electron sheaths can be present at boundaries. Electron sheaths are found when conductors are biased more positive than the plasma potential. A small probe biased much more positive than the plasma potential provides a small perturbation. But what is a small perturbation? The answer is somewhat surprising.

There are two sources of electrons in partially ionized hot cathode produced laboratory plasma, those injected into the plasma and those created by ionization of neutral gas within the plasma. In electrodeless rf produced plasma, all electron loss must be balanced by ion loss. The steady-state loss rate of ions must balance the loss rate of electrons created by ionization because ion and electrons are created with equal rates. The ion loss need not balance the injected electron current. Of course electrons lost at an electron sheath can be of either class.

It is tempting to argue that electron sheaths that extract a small fraction of the electron loss represent a small perturbation to the system. In fact, electron sheaths can extract all of the electrons lost from the system. The ratio of electron to ion flux associated with electrons created by ionization from Eqs. (11) and (16) is approximately equal to $\sqrt{m_i/m_e}$ if no potential dip is present. The limit to the size of the existence of an electron sheath is provided by the condition that the ion loss current be balanced by the electron loss current. Assuming all the electrons are lost at the electron sheath gives

$$\frac{A_i}{A_e} \approx \sqrt{\frac{m_i}{m_e}}, \tag{19}$$

where A_i and A_e are the ion and electron loss areas. For large A_e, the electron sheath is no longer a viable solution. The presence of a potential dip improves the situation. For sufficiently large A_e, only a plasma potential more positive than the positive electrode potential combined with an ion sheath can provide the necessary balance of electrons and ion losses.

III. SHEATH AND PRESHEATH MEASUREMENTS

Sheath plasma potential profiles are hard to measure. Electric fields in sheaths in many laboratory plasmas are the order or smaller than 100 V/cm or less and can have dimensions less than 1 mm. Langmuir probes provide a way to determine the properties of bulk plasma but they do not work in sheaths or presheaths. The equipotential contours near a Langmuir probe inserted in a sheath are shown in Fig. 1.[9] It is apparent that biasing the probe results in a large perturbation to the sheath structure and that electron saturation current will provide the bulk electron parameters rather than the local sheath/presheath parameters. We see that the probes tend to short out the sheath.

A. Emissive probes

Emissive probes have been a key diagnostic in our work. Operation of emissive probes in the limit of zero emission[10] is a diagnostic technique we developed to investigate weak electric fields and to distinguish between bulk and beam species. They provide a sensitive and relatively nonperturbing diagnostic of plasma potential with a resolution approaching 0.1 V and a spatial resolution of 0.1 cm. An emissive probe consists of an electron-emitting source whose potential can be varied. A simple version is a thermionically emitting hot wire (see Fig. 2). It provides a measurement of the plasma potential because electron emission is suppressed when the hot wire is biased more positive than the plasma potential, and electrons can be emitted when the wire is biased more negative than the plasma potential. Space charge surrounding the emitting wires reduces emission so that probes must be biased more negative than the plasma potential to emit. The basic idea of this technique is to extrapolate the inflection point to zero emission. An emissive probe was used to determine the equipotential contours shown in Fig. 1. The current

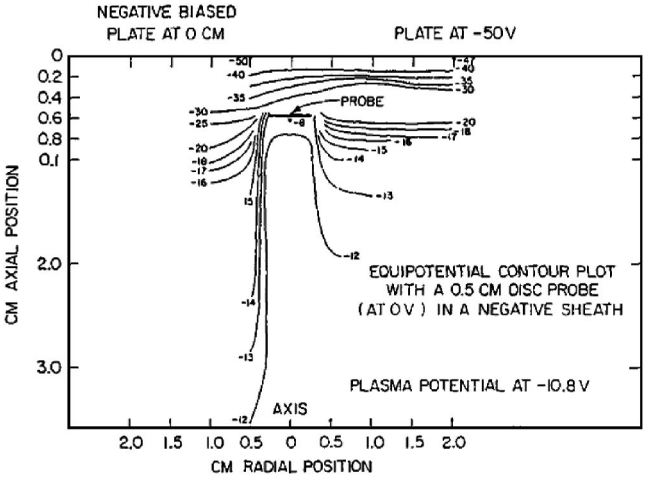

FIG. 1. Equipotential contours near a 0.5 cm diameter planar Langmuir probe biased at 0 V. The probe was positioned 0.6 cm from a plate biased at −50 V.

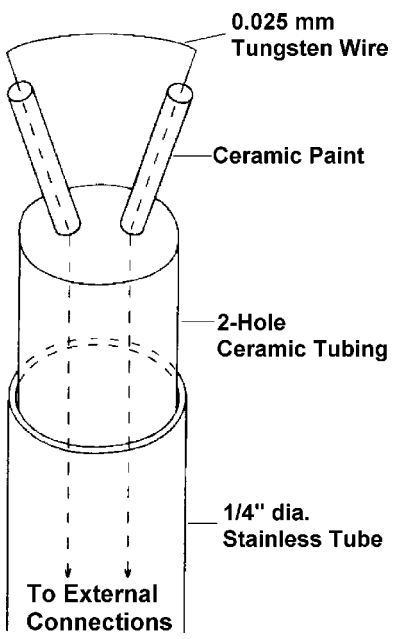

FIG. 2. Schematic diagram of an emissive probe.

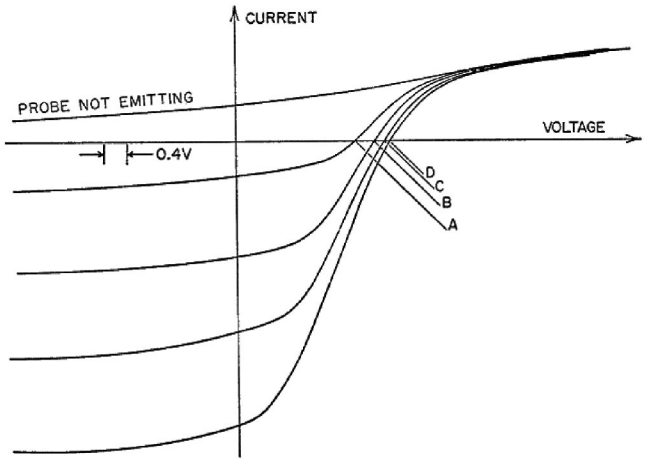

FIG. 3. Current-voltage curves for a heated wire probe. Curves A–D correspond to increasing heating voltage.

emitted into plasma by a hot wire vs the bias voltage on the wire is shown in Fig. 3. For low bias voltage the emitted current is space charge limited and given by the Child–Langmuir law. For sufficiently high negative bias voltage to the probe, the emitted current is given by the Richardson–Dushman equation

$$J_{\mathrm{th}} = AT^2 \exp\left(-\frac{eW}{T_w}\right), \tag{20}$$

where W is the work function. The current switches from electron current emission to current collection when the probe is biased more positive than the plasma potential as shown in Fig. 3. The curves all coincide in this regime. Differentiating the current vs voltage with respect to bias voltage gives the inflection point, i.e., the transition from emission to collection as seen in Fig. 4(a). Representative data showing the derivative of the current-voltage curves and the extrapolation to zero emission current are shown in Fig. 4(b). Over the years we have used emissive probes to determine the plasma potential in systems with plasma densities ranging from "vacuum"[11] to 10^{13} cm^{-3}, electron temperatures ranging up to 20 eV (Ref. 12) and neutral pressures up to 1 Torr.[13]

Experimental measurements were carried out using multidipole[14] "soup pot" plasma devices originally constructed out of stainless steel cooking pots[15] (see Fig. 5). Multidipole soup pots were employed in many of the experiments reported in this paper. Steady state plasma was produced by primary electrons, with energies the order of 60 eV, emitted from heated thoriated tungsten filaments. Primary electron confinement is enhanced by the surface multidipole magnetic field produced by permanent magnets.

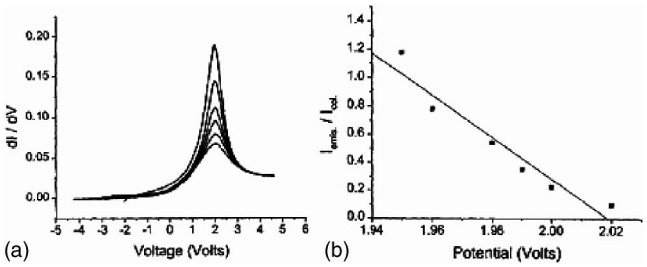

FIG. 4. (a) Derivative of emissive probe I-V characteristic curve. (b) Inflection point of I-V characteristic curve as a function of the ratio of the temperature limited emission current to the collected current.

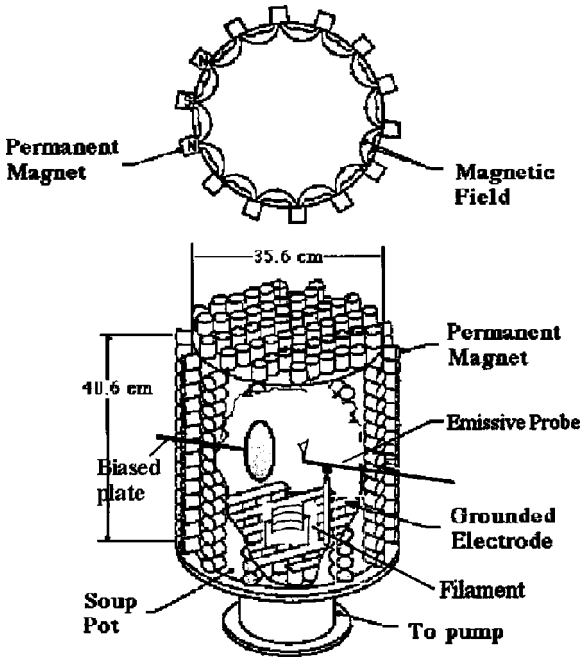

FIG. 5. Multidipole "soup pot" device. Alternating north and south line "cusps" provide a surface magnetic field.

B. Ion sheath data

The sheath at an electrode biased much more negative than the floating potential is an example of an ion sheath. The first measurements of the plasma potential associated with such a situation, measured in weakly ionized multidipole plasma, are shown in Fig. 6(a).[16] A closer look at the sheath shown in Fig. 6(c) shows that the Child–Langmuir

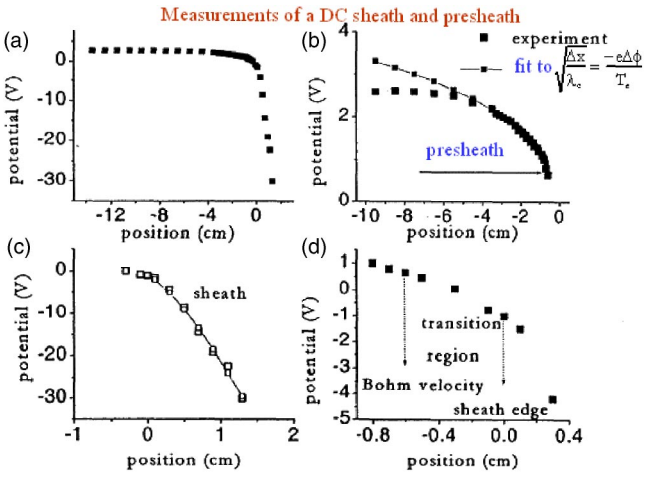

FIG. 6. Plasma potential profiles over (a) all of the plasma, (b) the presheath, (c) the "electron-free" sheath, and (d) the transition region of the sheath. Data are for 0.44 mTorr with a plasma electron density of 2.1×10^7 cm^{-3}. The lines show the fitted profiles.

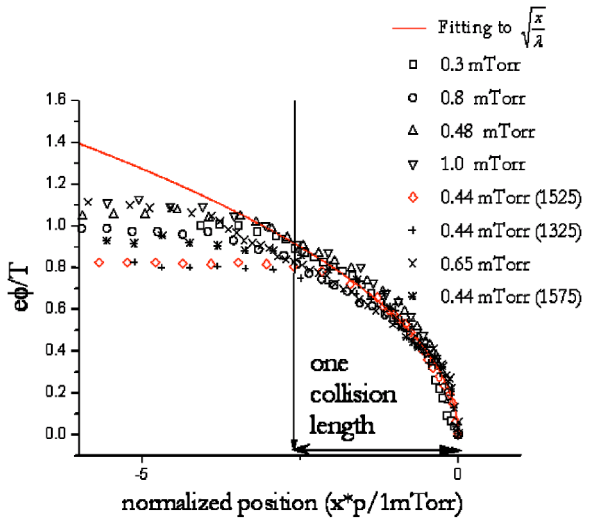

FIG. 7. Presheath plasma potential normalized to electron temperature vs distance from the sheath/presheath boundary multiplied by the neutral pressure. 0.44 mTorr data were measured for three combinations of filament heating voltage V_f and filament bias voltage V_b indicated by $V_f V_b$.

law is a good fit. Note that the fit is insensitive to the region where $eV/T_e \sim 1$. These data provide an opportunity to verify the assumptions used to derive Eq. (13) and to establish the characteristics of the presheath that accelerates ions to the Bohm velocity. Equation (15) is seen to be a good fit to the data in Fig. 6(b). The dependence of the presheath potential profile on neutral pressure is shown in Fig. 7. The dimensionless plasma potential data graphed vs x multiplied by pressure proportional to x/λ_c are all fit by Eq. (15). The parameters x_0 and ϕ_0 were determined from the best fits. After fitting the Child–Langmuir law to the sheath and Eq. (15) to the presheath in Fig. 6(b), a transition region was identified between the sheath and the presheath. Quasineutrality breaks down in this region. Note that the transition region thickness, found to be approximately $2\lambda_D$, is a significant fraction of the Child–Langmuir sheath width and the potential drop in the transition is comparable to the presheath potential drop [see Fig. 6(d)]. The fitting procedure underestimates the transition region thickness because the Child–

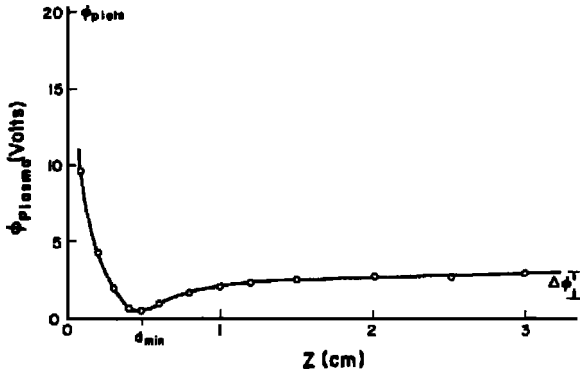

FIG. 9. Representative electron sheath near a plate biased at 20 V.

Langmuir sheath is assumed to start with zero electric field. The electric field in the transition region was found to be approximately equal to $T_e/e\lambda_D$ in agreement with the predictions of Godyak.

Collisions with neutrals become important for sheaths at higher neutral pressures. Emissive probe measurements of the sheath in a dc glow discharge given in Fig. 8 (Ref. 17) show the sheath is much broader than a Child–Langmuir sheath. Ion motion is described by mobility-limited flow.[18] In very collisional plasmas, the ion collision length λ_c can be much smaller than λ_D. For example, consider an argon plasma with $n=10^8$ cm^{-3}, $T_e=3$ eV, and neutral pressure $=10$ Torr. In such plasmas, there are only two relevant scale lengths, the plasma dimensions and the collision length. In this case, the bulk plasma takes on the role of the presheath that must be matched to a collisional sheath. The electric fields in the bulk plasma and sheaths are comparable and Bohm sheath criterion need not apply and the velocity at the wall may not reach c_s.

C. Electron sheath data

The plasma potential profile measured along the axis of a positively biased plate located in multidipole plasma shows the presence of an electron sheath as seen in Fig. 9.[19] A ceramic insulator covered the backside of the plate. When

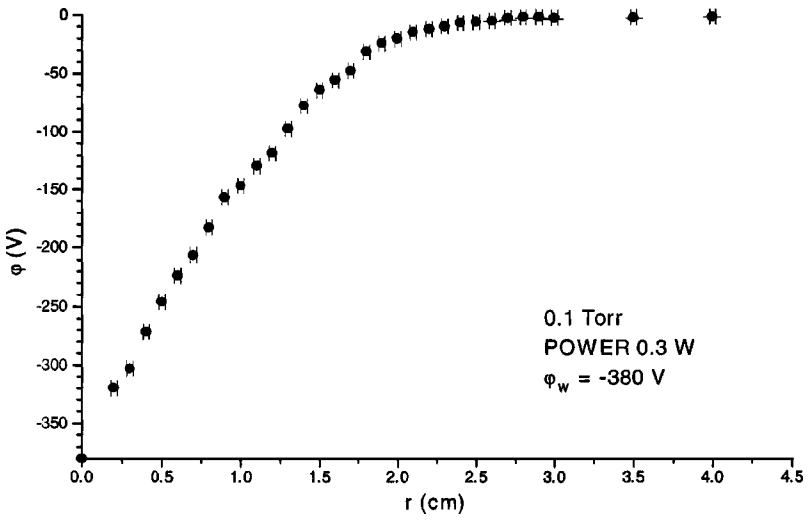

FIG. 8. Plasma potential profile of a dc glow discharge operated at 0.1 Torr.

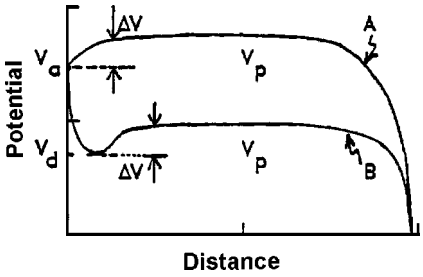

FIG. 10. Schematic of possible steady-state plasma potential profiles near a positively biased plate. Curve *A* corresponds to a large plate. Curve *B* corresponds to a small plate.

the insulator was removed, an electron sheath was not found and the plasma potential near the plate was more positive than the plate bias potential. This result is shown schematically in Fig. 10.[20] For curve *A* no insulator was present while for curve *B* the insulator was present. That result was attributed to the presence or absence of the insulator. Our recent measurements[21] have made it clear that the change in profile was the result of doubling the plate conducting area. Measurements of the plasma potential far (30 cm) from a biased plate at low pressure in another device given in Fig. 11(a) show that the bulk plasma potential remains unchanged with

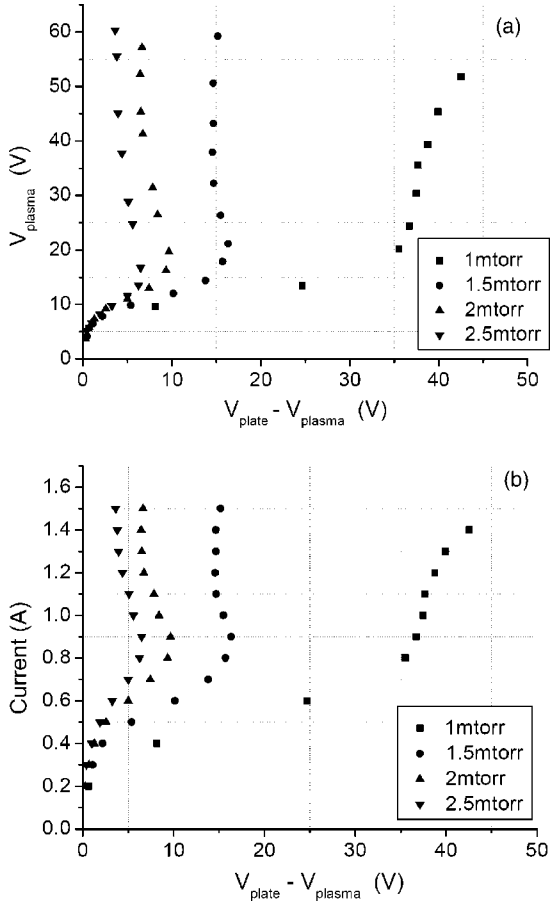

FIG. 11. The dependence of bulk plasma potential and plate current at an electron sheath on the plate bias voltage for five neutral pressures. The plate diameter was 5 cm and the filament emission current was 0.5 A. (a) Plasma potential vs $V_{plate}-V_{plasma}$. (b) Plate current vs $V_{plate}-V_{plasma}$.

increasing plate bias until a critical value is reached. Beyond this value, the potential drop across the electron sheath remains approximately constant by increasing the bulk plasma potential. The sheath width increases with increasing voltage drop across the sheath. With increasing neutral pressure the critical value of bias voltage moves to lower values. In Fig. 11(b), the current drawn by the plate for conditions corresponding to those of Fig. 11(a) are shown. The critical value of potential is seen to correspond to the condition that the plate draws the emission current from the filament.

The potential dip shown in Fig. 9 and Fig. 10 presents a problem in steady-state plasma.[22] Ion-neutral charge exchange in weakly collisional plasmas should fill up the potential dip. Charge exchange ions are electrostatically trapped in the well. The increased ion density reduces the curvature, i.e., the well depth. In steady state the dip should not exist. The solution appears to be that the potential dip seen in one direction is not a dip in the perpendicular direction, and that ions can leak out in the radial direction.[19]

The extremes of the plasma potential in rf plasma can be determined from the time-averaged emissive probe *I-V* characteristic curve. Peaks in the derivative dI/dV are found at maximum and minimum of the plasma potential. This is illustrated by data for a low-density inductive discharge shown in Fig. 12.[23] rf is applied to a spiral coil separated from the plasma by an electrostatic screen (Faraday shield) whose area could be varied (see Fig. 13). It is apparent that the minimum plasma potential is approximately constant near 20 V while the maximum varies linearly with the open area. Data near an electrode, to which a sinusoidal voltage is applied, in a filament produced multidipole plasma, is shown in Fig. 14.[24] Note that the maximum positive profile resembles the electron sheath profile including the potential dip shown in Fig. 9. The minimum potential profile resembles the ion sheath profile. Ion trapping in the potential dip is not a problem because charge exchange ions are emptied out each cycle. Overall, the characteristics of the potential dips are not understood.

IV. ACCELERATION AND "SHEATHS" AWAY FROM THE PLASMA BOUNDARY

Are presheaths the only way for ions to be accelerated to the Bohm velocity? In collisionless plasma it is not clear that the acceleration must take place in a region immediately adjoining the sheath. Schwager and Birdsall have provided an example of separation of the acceleration region from the sheath[25] in single ion species plasma. They modeled a Maxwellian source and absorbing plasma boundary using an electrostatic particle simulation code and found ions reach the Bohm velocity in the source sheath, obviating the need for presheath acceleration.

We have assumed sheaths occur at the plasma boundary. Do sheaths always occur at the boundaries? Two alternative wall plasma potential structures are shown in Fig. 15.[26] Double sheaths are well known near electron emitting surfaces.[27] Transient double layers have been identified as naturally occurring in magnetospheric plasma and both transient and steady-state double layers have been produced in

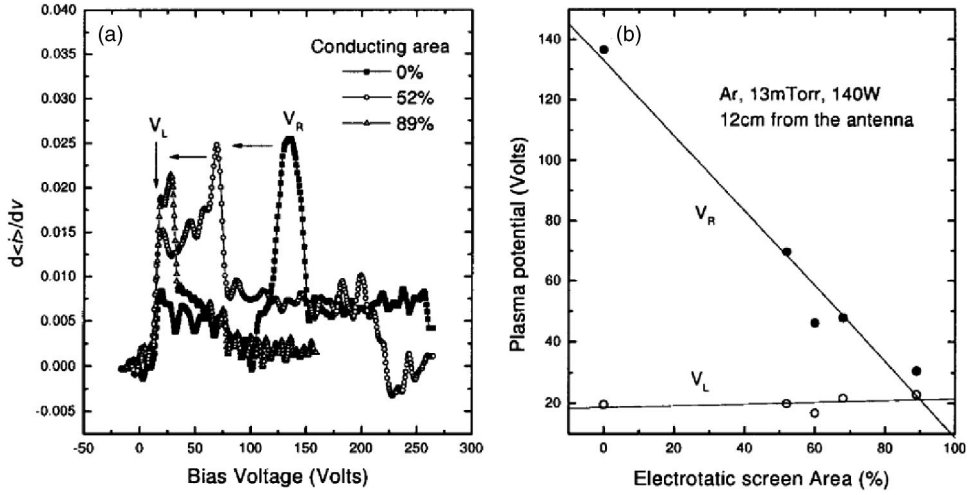

FIG. 12. (a) As the conducting area of the electrostatic screen is increased, the right-hand peak shows a decrease in the rf fluctuation amplitude. The left-hand peak is approximately constant. (b) Asymmetric behavior of the plasma potential with changing screen area. The lower limits of the plasma potential are almost constant.

laboratory plasma. Double layers are non-neutral regions located away from a plasma boundary that resemble an ion sheath connected to an electron sheath. They are typically several Debye lengths in thickness.

The plasma potential and ion and electron phase spaces for double layers and sheaths are shown in Fig. 16.[26] Trapped (reflected) and free particles determine the potential structure. Electrons (ions) are trapped for ion (electron) sheaths. Both electrons and ions can be trapped or free for double layers. Double layers have been observed when three of the four possibilities are present.[28] It is important to note that Poisson's equation does not depend on the direction of the particle velocities so free particles can enter the double layer from either side. Naturally occurring stationary double layers have not been identified near the walls of uniform plasma devices but no one has looked for them. However, naturally occurring double layers have been identified in nonuniform magnetized plasma.[29–31] Representative experimental double layers in which trapped and free particles are provided at plasma boundaries are shown in Fig. 17 (Ref. 32) and Fig. 18.[33] Ion acceleration can also be provided by combinations of several presheaths or double-layers. Multiple double-layer structures have been observed[34] in laboratory plasma (see Fig. 19), as have multiple presheaths[35] (although not in collisionless plasma).

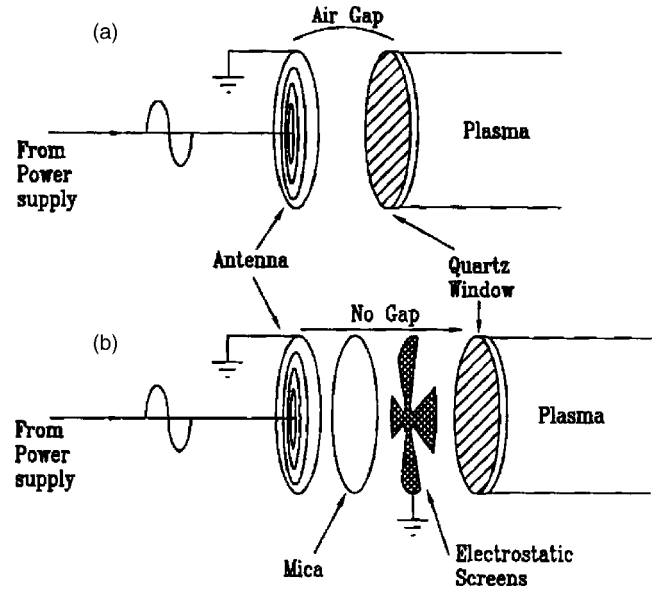

FIG. 13. A schematic drawing of the inductive source and the electrostatic (Faraday) screen.

V. MULTIPLE ION SPECIES

A. Theory

Most plasma encountered in industrial applications[18] or fusion studies consist of more than one-ion species. While many of the characteristics of the presheath are understood in

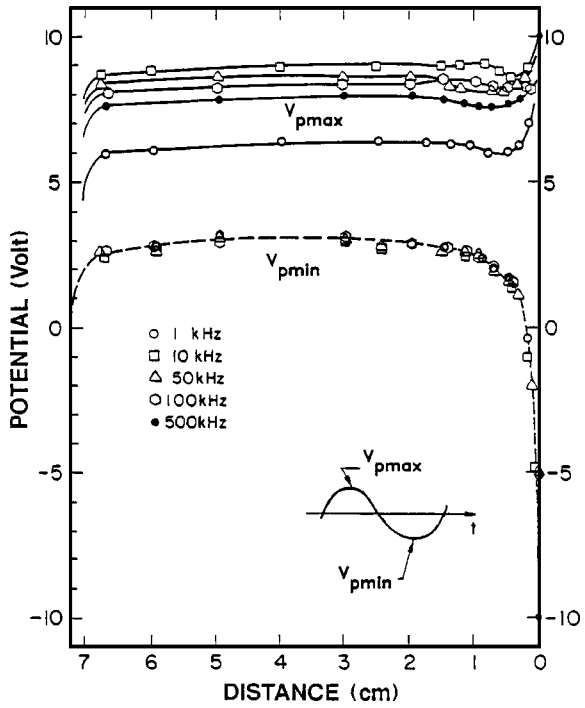

FIG. 14. Maximum and minimum plasma potentials profiles at different rf frequencies, measured by the time-averaged emissive probe technique. The applied rf was symmetric with respect to the ground. Plasma conditions were $n_e \sim 10^9$ cm^{-3}, $T_e \sim 2$ eV, $P_o \sim 10^{-4}$ Torr. The inset shows the times when the maximum and minimum plasma potentials occur.

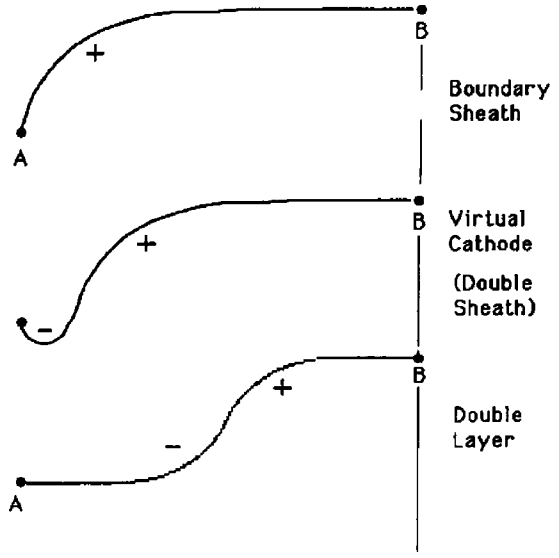

FIG. 15. Plasma potential profiles associated with three non-neutral structures: an ion sheath, a virtual cathode, and a double layer.

single species, this is not the case in multispecies plasma. The behavior of plasmas with two or more positive ion species is not a simple extrapolation from single positive ion species plasma. Mobility limited flow cannot provide the Bohm velocity or close to the Bohm velocity for each species and it is not clear that each ion species should reach those velocities.

In the presence of multiple-ion species, Riemann has derived a generalized Bohm criterion that must be satisfied at the sheath/presheath boundary.[36] Assuming collisionless, instability-free one-dimensional motion, conservation of ion energy and flux at sheath/presheath boundary and Boltzmann electrons gives

$$\frac{\partial n_i}{\partial \phi} = \sum_j \frac{n_{j0} e}{m_j v_{j0}^2} \left(1 - \frac{2e\phi}{m_j v_{j0}^2}\right)^{-3/2} \tag{21}$$

and

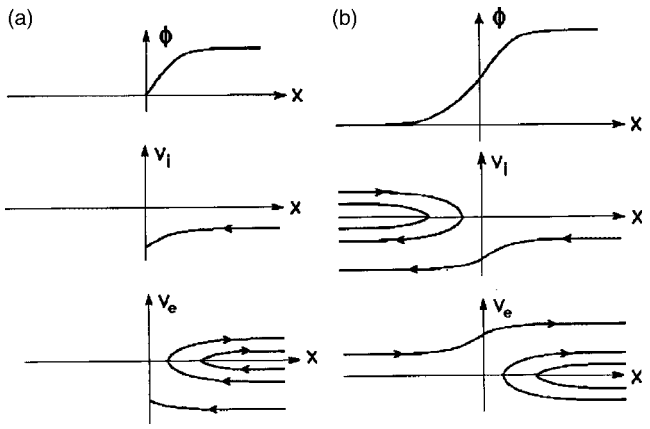

FIG. 16. Plasma potential profiles and ion and electron phase space associated with (a) an ion sheath and (b) a double layer.

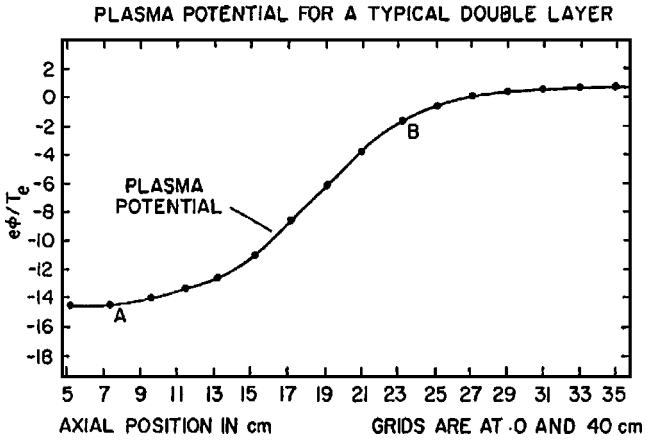

FIG. 17. A typical potential plot for double layers as measured by an emissive probe. Planar Langmuir probes do not provide a good measurement of the plasma potential over the region between *A* and *B*. Outside *A* and *B*, the emissive and collecting probes are in good agreement.

$$\frac{\partial n_e}{\partial \phi} = \frac{e}{T_e} n_{e0} \exp\left(\frac{e\phi}{T_e}\right). \tag{22}$$

Equating Eqs. (21) and (22) at the sheath/presheath boundary, where $\phi \equiv 0$ gives Riemann's generalized Bohm criterion for a system of multiple-ion species (here assumed to all be singly charged)

$$\frac{n_{e0}}{T_e} \geqslant \sum_j \frac{n_{j0}}{m_j v_{j0}^2}. \tag{23}$$

It is important to observe that this criterion depends explicitly on the all species velocities at the sheath edge. The velocities of individual species are not specified. Although an infinite number of solutions exist, two interesting ones are the following:

$$\text{Solution 1, } \frac{1}{v_{j0}^2} = \frac{1}{c_{sj}^2} \approx \frac{m_i}{T_{e0}}, \tag{24}$$

assuming $T_i \ll T_e$, and

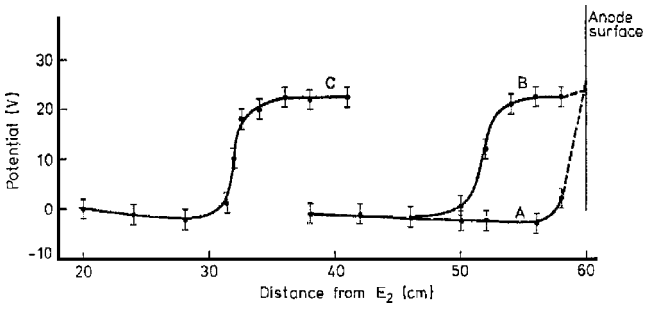

FIG. 18. Double layers corresponding to different discharge conditions. Curve *A* shows the potential profile along the column before the double-layer formation when an electron (anode) sheath is present. Curves *B* and *C* show double-layer corresponding to two different discharge currents.

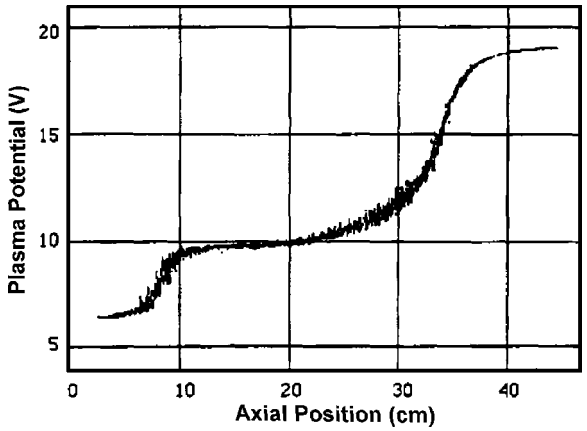

FIG. 19. Plasma potential vs axial position of a two-step double layer.

Solution 2, all ions have the same velocity v_s at the sheath/presheath boundary

$$v_s^2 \geqslant \sum_j \frac{n_j}{n_{e0}} \frac{T_{e0}}{m_j} = \sum_j \frac{n_j}{n_{e0}} c_{sj}^2. \tag{25}$$

For solution 1, each ion species is lost at its own Bohm velocity while for solution 2, all species are lost at the same velocity v_s which equals the sound velocity of the system of particles. In the presence of weak collisions and instabilities, it is not clear whether solution 1 or 2 or perhaps another solution describes the losses from a multi-ion system. Solution 1 is somewhat attractive because if ions are born with the same spatial profiles, they might be able to pick up the same kinetic energy in falling through the presheath potential. However, in real plasma the assumption of collisionless, instability-free one-dimensional motion is not realistic. Charge exchange, other ion-neutral collisions, different species ionization rates, and streaming instabilities in real plasma all can affect the first solution.

B. Laboratory experiments

The presheath/sheath boundary near a negatively biased plate in a multidipole plasma was identified as the position where a significant change occurred in the plasma potential measured by an emissive probe. Laser induced fluorescence (LIF) measurements were made of the argon ion velocity distribution function in argon plasma using a diode laser.[37] The data given in Fig. 20(a) demonstrate that the Ar^+ ions reach their Bohm velocity at the sheath edge as expected. LIF measurements in a two-species (argon+helium) plasma, given in Fig. 20(b), demonstrate that the Ar^+ ions reach their Bohm velocity before reaching the sheath edge. The generalized Bohm condition could then be satisfied with He^+ ions moving slower than their Bohm velocity at the sheath boundary but the assumptions used to derive the generalized Bohm condition are questionable.

VI. INSTABILITIES

The drift velocities of the two-ion species differ throughout the presheath although they might be the same at the presheath/sheath boundary. The velocities differ by less than the individual species Bohm velocities. This ion distribution function is ion-ion two-stream unstable.[38] The frequency spectra of ion saturation current to a negatively biased cylindrical probe are shown in Figs. 21(a) and 21(b) as a function of the neutral concentration of Ar added to a He plasma. As seen in Fig. 22(a), the instability frequency increases with the addition of argon. This behavior is qualitatively consistent with the predictions of the appropriate ion fluid and kinetic equations shown in Fig. 22(b). Note that different scales are used for the theory and data. The linear growth rates calculated for the instabilities shown in Fig. 22(b) are relatively small and unlikely to make significant changes in the ion distribution functions. The Ar^+/He^+ ratio does not equal the Ar/He ratio of the neutral species because of Penning ionization of the Ar via He metastables.[39] The Ar^+ and He^+ concentrations in the bulk plasma were determined from the phase velocity of ion acoustic waves launched in the bulk plasma region.[40] The concentrations in the presheath were not corrected for the effects of ion acceleration (and the corresponding density reduction) or charge exchange.

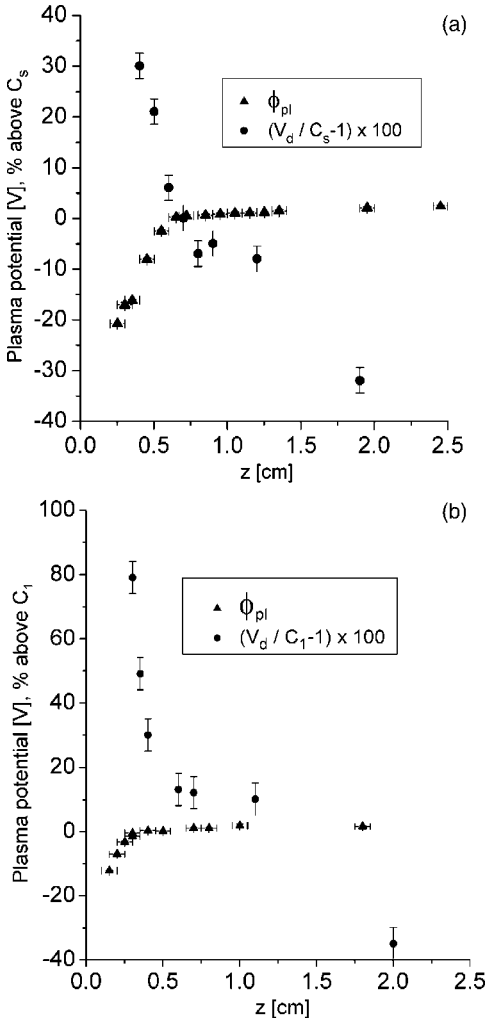

FIG. 20. (a) The spatial profiles of the plasma potential and ion drift velocity determined by LIF in an Ar plasma. C_s is the argon ion Bohm velocity. (b) The plasma potential and drift velocity profile for Ar^+ in an Ar+He plasma. C_1 is the argon ion Bohm velocity.

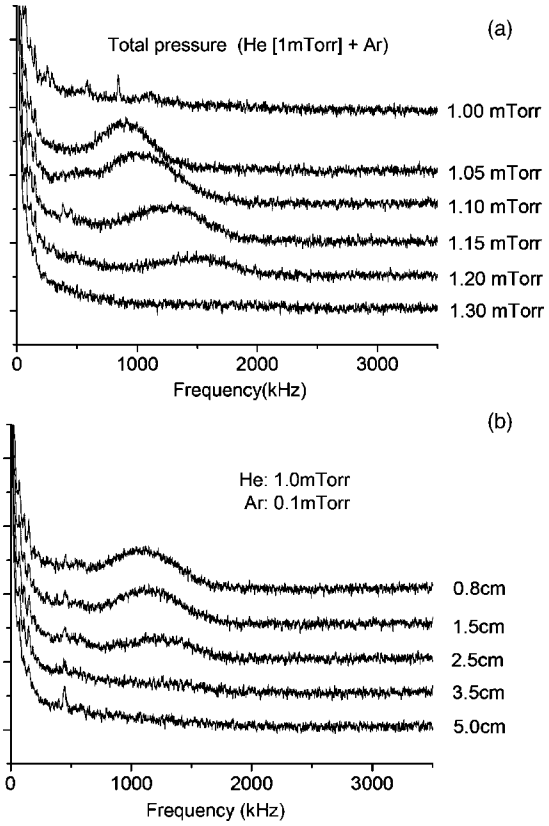

FIG. 21. Log of power spectra measured from fluctuations in ion saturation current as a function of (a) the addition of Ar to a 1 mTorr He plasma and (b) the distance from the wall with 0.1 mTorr Ar and 1 mTorr He plasma. Curves are displaced vertically for clarity.

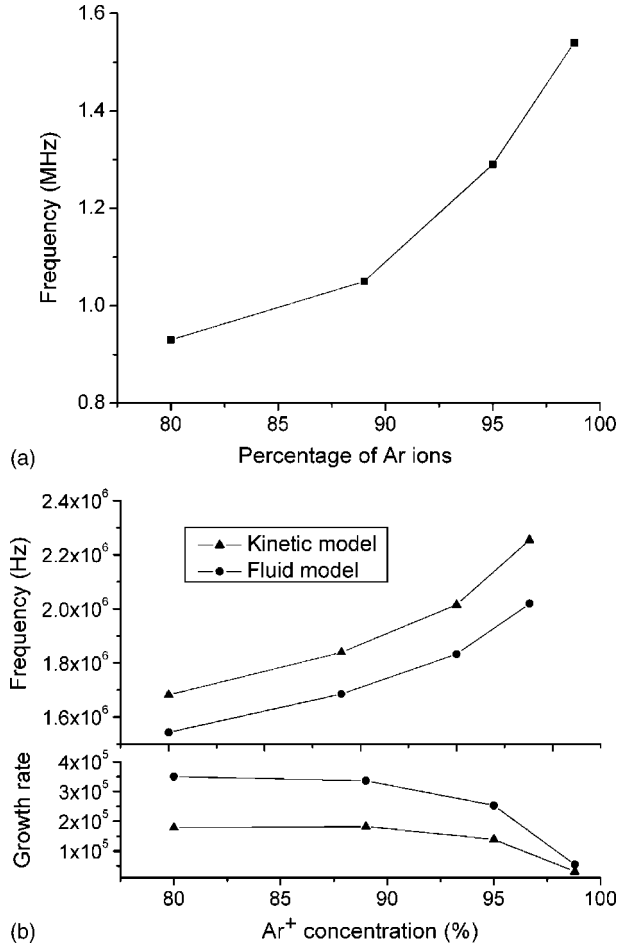

FIG. 22. (a) The peak frequency observed in Fig. 21 vs Ar^+ concentration. (b) Frequencies and growth rates predicted by fluid and kinetic equations.

VII. CONCLUSIONS

Overall, ion sheaths in single-ion species weakly collisional plasma with $eV/T_e \gg 1$ are better understood than electron sheaths. Both ion and electron sheaths can exist and the Child–Langmuir law provides good fits to potential vs position when $eV/T_e \gg 1$. Electron sheaths are much less common than ion sheaths because they require that a sufficient area be available in the plasma chamber for the ion loss current and many chambers are not big enough. The characteristics of potential dips preceding many electron sheaths are not well understood.

In weakly collisional plasmas, most of the ion acceleration to the sheath boundary takes place in a presheath within a collision length λ of the boundary. Emissive probe data show the plasma potential in the presheath varies as $e\phi/T_e = \sqrt{x/\lambda}$, measured from the sheath/presheath boundary in agreement with Riemann's predictions. When $eV/T_e \gg 1$, the Child–Langmuir sheath provides a good fit. A transition region, the Debye sheath, in which the ion density becomes negligible is found between the presheath and Child–Langmuir sheath, so sheaths are normally thicker than the Child–Langmuir sheaths. The electric field in the transition region is found to be $E \approx T_e/e\lambda_D$ in agreement with the qualitative predictions of Godyak. LIF data indicate $v \approx c_s$ at the presheath/sheath boundary for single species plasma. Both electron and ion sheaths are seen in rf plasmas. Double layers provide a way for a "sheath" to form away from the boundary.

More than one ion species are present in most plasmas of interest, but sheaths and presheaths of multiple species plasma are not well understood. LIF data indicate $v_{Ar} > c_s$ at the presheath/sheath boundary for an $Ar^+ - He^+$ plasma and it is not clear how the individual ion velocities are determined. Furthermore, the presheath was shown to be ion-ion unstable. The multiple species presheath/sheath problem still needs lots of work.

ACKNOWLEDGMENTS

The author is grateful to Eunsuk Ko for assistance in preparing this paper.

This work was supported by the Department of Energy Grant No. DE-FG02-97ER5447.

[1] F. F. Chen, *Introduction to Plasma Physics and Controlled Fusion*, 2nd ed. (Plenum, New York, 1974), Chap. 8.
[2] Irving Langmuir, Phys. Rev. **33**, 954 (1929).
[3] D. Bohm, *The Characteristics of Electrical Discharges in Magnetic Field*, edited by A. Guthrie and R. K. Wakerling (McGraw-Hill, New York, 1949), Chap. 3.
[4] P. C. Stangeby and A. V. Chankin, Phys. Plasmas **2**, 707 (1995).
[5] D. J. Koch and W. N. G. Hitchon, Phys. Fluids B **1**, 2239 (1989).
[6] G. A. Emert, R. M. Wieland, A. T. Mense, and J. N. Davidson, Phys. Fluids **23**, 803 (1980).

[7]K. U. Riemann, Phys. Plasmas **4**, 4158 (1997).
[8]V. A. Godyak, Phys. Lett. **89A**, 80 (1982).
[9]P. Coakely, Ph.D. dissertation, University of Iowa, 1980.
[10]J. R. Smith, N. Hershkowitz, and P. Coakley, Rev. Sci. Instrum. **50**, 210 (1979).
[11]M. H. Cho, C. Chan, N. Hershkowitz, and T. Intrator, Rev. Sci. Instrum. **55**, 631 (1984).
[12]N. Hershkowitz, B. Nelson, J. Pew, and D. Gates, Rev. Sci. Instrum. **54**, 29 (1983).
[13]S. Yan, H. Kamal, J. Amundson, and N. Hershkowitz, Rev. Sci. Instrum. **67**, 4130 (1996).
[14]R. Limpaecher and K. R. Mackenzi, Rev. Sci. Instrum. **44**, 726 (1973).
[15]K. N. Leung, T. K. Samec, and A. Lamm, Phys. Lett. **51**, 490 (1975).
[16]L. Oksuz and N. Hershkowitz, Phys. Rev. Lett. **89**, 145001 (2002).
[17]Husain Kamal, Ph.D. dissertation, University of Wisconsin, 1997.
[18]M. A. Lieberman and A. J. Lichtenberg, *Principles of Plasma Discharges and Materials Processing* (Wiley, New York, 1994), materials found throughout the book.
[19]C. Forest and N. Hershkowitz, J. Appl. Phys. **60**, 1295 (1986).
[20]M-H. Cho, N. Hershkowitz, and T. Intrator, J. Appl. Phys. **67**, 3254 (1990).
[21]S. Baalrud (private communication).
[22]N. Hershkowitz, C. Forest, E. Y. Wang, and T. Intrator, Laser Part. Beams **5**, 257 (1987).
[23]T. Lho, N. Hershkowitz, G. H. Kim, W. Steer, and J. Miller, Plasma Sources Sci. Technol. **9**, 5 (2000).
[24]M-H. Cho, N. Hershkowitz, and T. Intrator, J. Vac. Sci. Technol. A **6**, 2978 (1988).
[25]L. A. Schwager and C. K. Birdsall, Phys. Fluids B **2**, 1057 (1990).
[26]N. Hershkowitz, IEEE Trans. Plasma Sci. **22**, 11 (1994).
[27]T. Intrator, M-H. Cho, E. Y. Wang, N. Hershkowitz, D. Diebold, and J. DeKock, J. Appl. Phys. **64**, 2927 (1988).
[28]N. Hershkowitz, Space Sci. Rev. **41**, 351 (1985).
[29]E. E. Scime, P. A. Keiter, M. W. Zintl *et al.*, Plasma Sources Sci. Technol. **7**, 186 (1998).
[30]S. A. Cohen, N. S. Siefert, S. Stange *et al.*, Phys. Plasmas **10**, 3804 (2003).
[31]C. Charles and R. W. Boswell, Phys. Plasmas **11**, 1706 (2004).
[32]P. Coakley and N. Hershkowitz, Phys. Fluids **22**, 1171 (1979).
[33]S. Torven and D. Anderson, J. Phys. D **12**, 717 (1979).
[34]A. Bailey and N. Hershkowitz, Phys. Fluids **25**, 2135 (1982).
[35]G.-H. Kim, N. Hershkowitz, D. A. Diebold, and M.-H. Cho, Phys. Plasmas **2**, 3222 (1995).
[36]K. U. Riemann, IEEE Trans. Plasma Sci. **23**, 709 (1995).
[37]G. D. Severn, X. Wang, E. Ko, and N. Hershkowitz, Phys. Rev. Lett. **90**, 145001 (2003).
[38]A. M. Hala, Ph.D. dissertation, University of Wisconsin, 2000.
[39]G. Hairpetian and R. L. Stenzel, Rev. Sci. Instrum. **58**, 2099 (1987).
[40]A. M. Hala and N. Herskowitz, Rev. Sci. Instrum. **72**, 2279 (2001).